EXPERIMENTAL AND NUMERICAL STUDY OF THE DOUBLE STAGE BURNER WITH VORTEX GENERATOR

Abay DOSTIYAROV[1], Jordan HRISTOV[2], Zhanat OZHIKENOVA[3, *], Viacheslav POLOVNIKOV[4], Bauyrzhan NAURYZ[1], Nellya JAMANKULOVA[1, *]

[1] G.Daukeev Almaty University of Power Engineering and Telecommunications, Almaty, Kazakhstan

[2]University of Chemical Technology and Metallurgy, Sofia, Bulgaria

[3]NJSC «S. Yessenov Caspian University of Technologies and Engineering», Aktau, Kazakhstan

[4]National Research Tomsk Polytechnic University, Tomsk, Russia

[*] Corresponding authors; E-mails: ozhikenova92@mail.ru, jnelya@gmail.com

Systematic studies of a double-tier (double-stage) combustion device allowing an effective combustion process due to controlled fuel excess independently in the tiers have been reported. The investigations reported stress the attention on the relationship of the NO_x and CO emissions to the air excess and demonstrate that there is an optimal range of air supply minimizing them. A mathematical model allows numerical studies on the novel combustion device and reveals the contributions of the combustion processes carried out in each tier to the gross performance of the combustion device.

Keywords*: double stage burner, combustion, NOx, CO, angle of the vortex generator*

1. Introduction

The contemporary approaches in combustion processes of both liquid and gaseous fuels and related emissions of NOx [1-3] demonstrate that the existence of recirculation zones for fuel-air mixing results in argumentation of the combustion process efficiency. In this context, for instance, a simultaneous supply of air-water vapor mixture to both inner and outer ring channels of the combustion chamber allows reduction of NOx emission down to на 55% when diesel fuel is used [1]. From another point of view, the effect of flow vortices on the NOx emissions in double-stage combustors with preliminary preheating utilizing flue gases has been systematically studied [2]. The increase in the angle of the vortex generator with 5°, for instance, yields a reduction in NOx concentration down 104.47 ppm. In this context, tests with Jet-A1 fuel with a two-stage combustion process resulted in a minimal concentration of NOx upon conditions imposed by $\varphi = 0.18$, but with increased emission of CO [3].

Studies of a double stage combustor [4] demonstrated that the increase in the vortex angle of the outer swirler up to $20 - 30^o$ an allowed reduction in the needed air supply with about 37% as well as yields 25% reduction of NOx emissions. Moreover, the addition of argon, helium, and carbon dioxide [5] demonstrated that in the case of double-stage combustion the reduction in the NOx

emissions could attain down 16 ppm, and the angles of the vortex generators (swirlers) play crucial roles in the process of combustion process efficiency parallel to fuel excess ratio [6].

The modern engine based on gas combustion turbines utilizes various frontal combustion chambers with blade stabilizers, impinging-vortex flows, micro modular flares, air-supported stabilizers, etc. [6-10]. In such devices, there micro modular flare combustion processes take place [6-10]. In this context, we have to mention the combustion chambers with zonal burning [11] where the gaseous fuel is supplied as axial, radial, or circulation flows. The double-stage fuel combustion allows the development of devices and processes with low dangerous emissions and allows the reduction of the combustion chamber length by about 30%.

Double-stage and multistage combustion processes address the organization of the process as consequent discrete zones [17] mainly as radial-circular distribution with zonal premixed fuel-air supply [12-18] resulting in a strong reduction in the NOx emissions [18-24, 26].

This research was carried out on a newly developed burner device (device detailed depiction is given in [25]), for which experimental and numerical studies were carried out.

This work presents experimental results and numerical simulations of double-stage combustion devices with swirler' blade variations allowing control of the combustion process efficiency and NOx emissions.

2. Experimental setup

The experimental set-up is shown schematically in Fig. 1, while photos of the double-stage (double-concentric swirlers) chambers are shown in Fig. 2. The set-up consists of air supply by a fan, fuel supply and measuring devices.

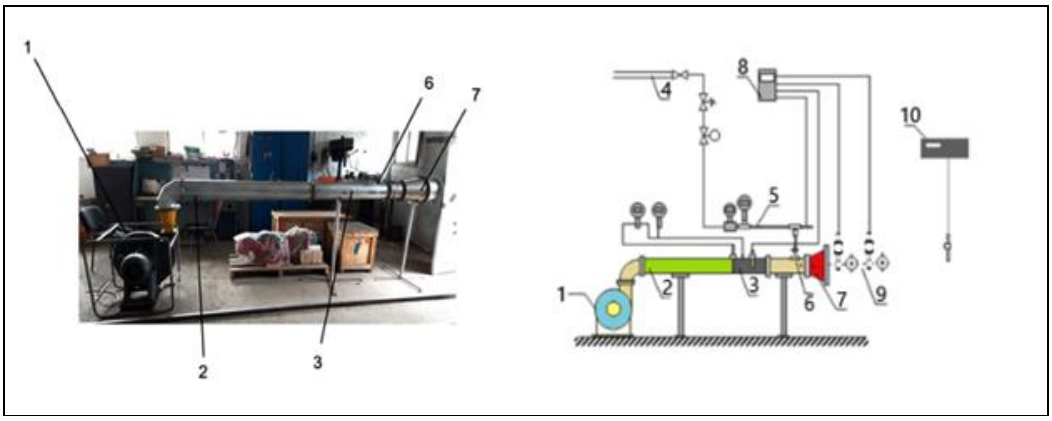

Figure 1. Experimental set-up: 1 – fan; 2 – stabilizing flow tube bundle; 3 – measurement point at the flow entrance; 4 – gas flow supply; 5 –measurement point for fuel supply; 6 – fuel supply tube; 7 – front diffusor with the combustion device; 8 –multichannel data acquiring system; 9 – measurement point behind the diffusor; 10 – gas analyzer

The air supplied by the fan initially passes through a stabilization tube 2 (20 cm ID and 1.9 m long) allowing flow field to be almost homogeneous at the entrance of the double-stage chamber 7. The air flow is measured by anemometer (testo 410-2) and air parameters measuring device 3, both of them connected in a series with the stabilization tube. The general view of the combustion device is

shown in Fig. 3. The gaseous fuel from the main gas fuel tract is supplied by the pipe 6 assembled with a flow meter 5.

The experiments were oriented towards the determination of the impact of the operating regimes on the emissions of NOx and CO, as well as the flame detachment and the stabilization characteristics of the combustion process. The angles of the blades of the two swirlers were established at 45^o. The airflow varied in the range from 2 up to 6 m/s, supplied by a high-pressure fan (BP120-28-5,2C-01) and was controlled by anemometer and its mass flow was corrected with changes in the temperature (measured by standard chrome-alumel thermocouples with accuracy) and pressure. The pressure drop was measured by a manometer Metran-100-1411 (accuracy class 0.5). The concentrations of NOx and CO in the exhaust gases were measured by a gas analyzer (Testo 350-XL), parallel to temperature measurements by Chrome-Alumel thermocouples (positioned symmetrically concerning the combustion chamber symmetry axis). The pressure of the fuel supply was measured by a manometer (MP50M, Russia) with an accuracy class of 2.5.

The fuel used was liquefied propane, supplied from a container (5 liters) upon the pressure of 1.57 MPa and the flow was controlled by a valve allowing maintaining the fuel mass flow up to 4 g/s

2.1. Combustion device

The combustion device (see Fig. 2) was designed as a double-swirler (two-row swirler or double-tier) microflare burner, with 45^o blade angle (of both tiers).

Electric spark igniter was located just after the swirlers at the symmetry axis.

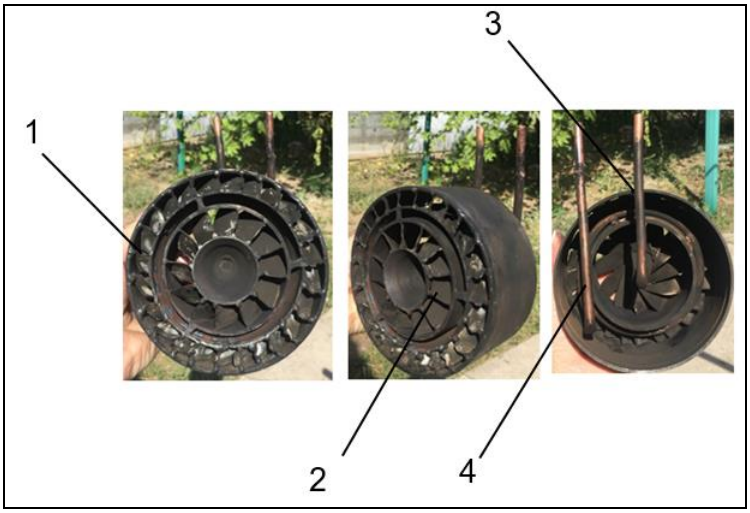

Figure 2. General view of the combustion device: 1–Outer swirler, 2–Inner swirler; 3–fuel supply tube for the inner swirler, 4 – fuel supply tube for the outer swirler

2.2. Numerical modeling

The numerical modelling utilized the same parameters of the process as in the experiemental run that allowed comparing the simulation procedure efficiency and the adequacy of the modelling approach. The schematic picture used in the ANSYS modelling is shown in Fig. 5. The $k-\varepsilon$ turbulence model (with turbulence intensity in the range $2-5\%$) and non-premixed combustion model, by the analogy of similar studies [1, 2, 4, 20] were applied.

The simulation was based on the combustion of propane (C_3H_8) assuming the ambient temperature 288 K. The hydraulic diameter of the combustor varies from 0.115 up to 0.120 m with changes in the angles of the swirler blades.

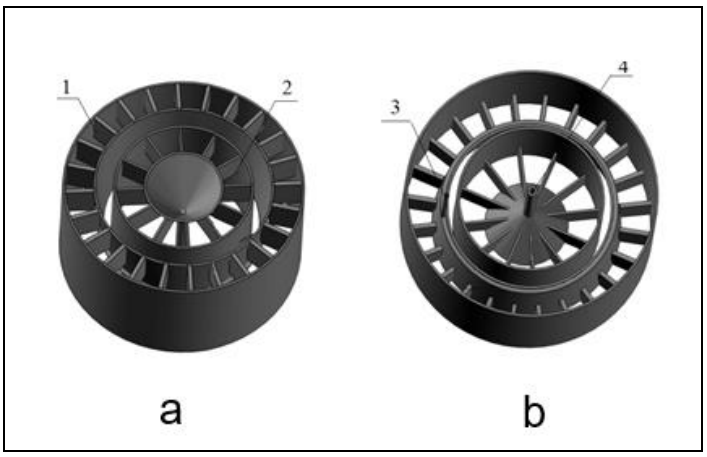

Figure 3. Physical model of the two-row swirler combustor studied: a – frontal view; b – backside view; 1 – outer swirler, 2 – inner swirler; 3 – fuel supply for the outer swirler; 4 – fuel supply for the inner swirler

2.3. Mathematical model

The governing equation in accordance with the k-ε turbulence models [6] are

Continuity equation:

$$\frac{\partial p}{\partial t}+\frac{\partial\left(pu_i\right)}{\partial x_i}=0 \tag{1}$$

Momentum equation:

$$\frac{\partial\left(\rho u_i u_j\right)}{\partial x_j}=-\frac{\partial\left(p\right)}{\partial x_i}+\frac{\partial \tau_{ij}}{\partial x_j} \tag{2}$$

Energy equation:

$$\frac{\partial\left(\rho u_i h\right)}{\partial x_i}=\frac{\partial}{\partial x_i}\left(\lambda_f \frac{\partial T}{\partial x_i}\right)+\sum_j\left[\frac{\partial}{x_i}(D_{j,m}\rho h_j \frac{\partial Y_j}{\partial x_j})\right]+q \tag{3}$$

where h is the total enthalpy of mixture gas, h_i is the enthalpy of component j^{th} , λ_f is the thermal conductivity of the fluid, and q is the heat of reaction [15].

State of ideal gas:

$$p=\rho RT\sum_{s=1}^{Ng}\frac{Y_s}{M_s} \tag{4}$$

The numerical simulation runs reveal strong effects of the related heat transfer, mainly heat exchange between solids and gases [22-24]. Taking into account that heat conductivity of steel (the bluff body construction) was accepted as $42.5\ W/m\cdot K$. Thus, the energy equation for the solid parts in a steady-state is :

$$\frac{d\left(k_s dT\right)}{dx^2}+\frac{d\left(k_s dT\right)}{dy^2}=0 \qquad (5)$$

2.4. Numerical solutions: Grid independence study

To confirm the numerical simulation, we compared the experimental results with the calculation results. The dimensions of the combustion chamber model are the same as in experimental studies. The average gas temperatures at the outlet of the combustion and simulation chamber are shown in Figure 9. A temperature comparison shows good convergence. The Table 1 shows the following boundary conditions used in the study. To save the calculation time, we used grids with sizes of 2, 3, and 6 mm (the relevant information is summarized in Table 2). Additional information about the physical situations simulated is presented in Table 3.

Table 1. **The boundary conditions for numerical simulations**

	Temperature, K	Pressure, kPa	Velocity, Flow rate	Hydraulic diameter, m	Turbulence intensity, %
Air inlet	288	0	4 m/s	0.115	2
Fuel inlet	288	30	0.001 kg/s	0.021	5
Outlet	288	0	-	0.12	2

To confirm the obtained data, we compared the obtained temperatures at the outlet of the experimental setup and the results of numerical simulation for β = 60˚. The comparison results are presented in Table 2. The difference in the data obtained does not exceed 14%. Additionally, a comparison of the concentration of nitrogen oxides was carried out.

Table 2. Grid independence study results

№	Grid	Element numbers	Outlet Temperature (simulation) $T_{sim.}$, K	Outlet Temperature (experiment) T_{exp}, K	Difference, % $100\ x(T_{exp}-T_{sim})/\ T_{exp}$
1	2 mm	1531546	338	324	4%
2	3 mm	1111283	352		8.6%
3	6 mm	874351	365		12%

3. Results and Discussion

The experimental results (see Fig.4) reveal strong effects of the fuel excess supply on the formation of NOx. The plots clearly show that behind the inner swirler the emissions of NOx are

lower and this can be attributed to the strong intensity of flow vortices generated by this element of the combustor. In contrast, the NOx behind the outer swirler is greater mainly due to the lower vortex intensities generated by this section. In general, the increase in the intensity of fuel-air mixing results in augmented combustion process efficiency with high process temperatures and therefore increased formations of NOx. In the same context, the increase in the excess of fule supply yields increased NOx emissions by both inner and outer swirlers.

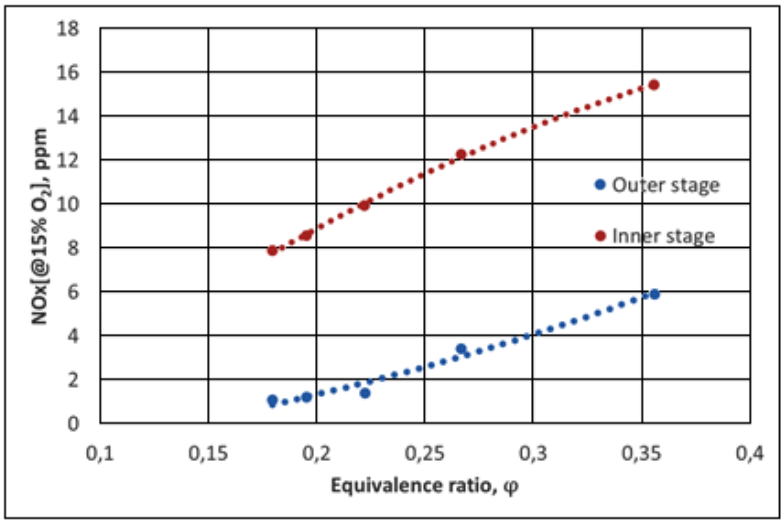

Figure 4. NO_x emissions as a function of the excess

The emissions of CO of the fuel supply excess upon the same experimental conditions as in Fig. 4 are shown in Fig. 5. In general, the maxium of CO was detrected in the zome where the fuel concentaqtion is minimal and this can be attributed to incomplete combustion. In this context, it is noteworthy that in the outer swirler the process of incomplete combustion takes place to a greater extent due to greater fuel supply in this section of the combustor.

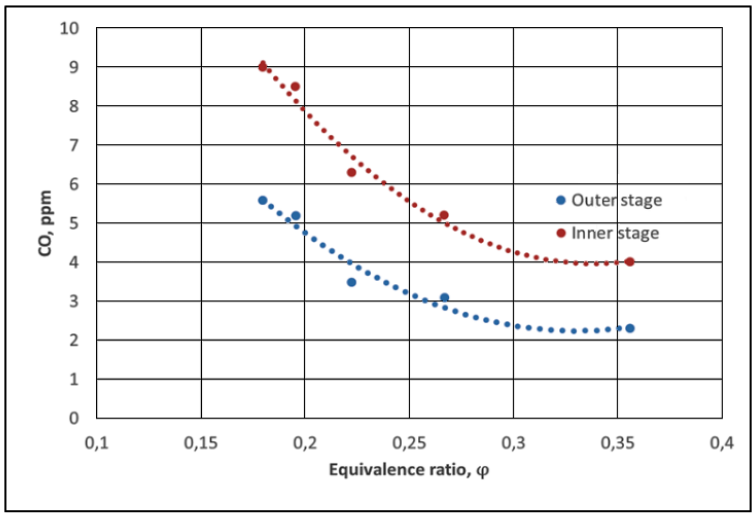

Figure 5. CO emissions as a function of the fuel excess

The temperature profiles in both the inner and outer swirlers shown in Fig. 6 reveal the effect of the air excess. In general, the maxima in the temperature are attained when the fuel excess is maximal. These results are strongly related and confirm, the effects attributed to the NOx and CO emissions. With a reduction in the air supply the consequent reduction in the temperature due to incomplete combustion.

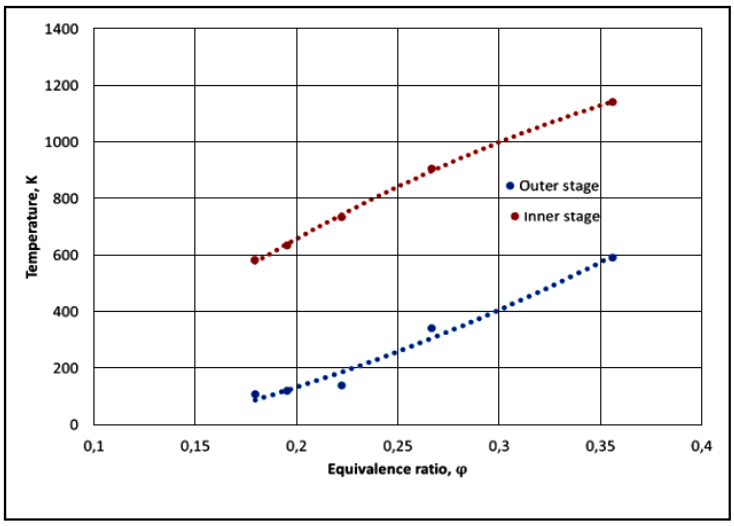

Figure 6. Tempeature evolution as a function of the air excess

The photos in Fig.7, in both the inner and outer swirlers, allow seeing what is the reality of the combustion process when the blades are inclined at 45^o. It is noteworthy to stress the attention that 45^o of blade inclination assures the maximal level of swirling of flow fields and fuel-air mixing. When the coefficient of fuel excess φ is minimal there is incomplete combustion and the flame is practically invisible. With the increase in the fuel concentration, the stoichiometric conditions are gradually attained and then the combustion is performed by a blue flame.

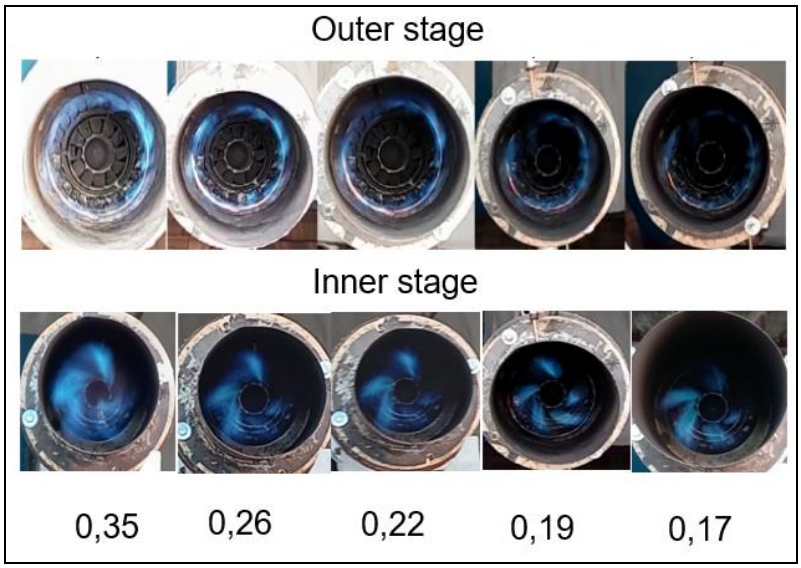

Figure 7. Photos of the combustion process in a double row swirler combustor

The bad fuel failure, represented by the equivalence ratio φ, strongly depends on the airflow rate as is illustrated by the plots in Fig. 8 concerning the process in the inner swirler. In general, the inner swirler is more stable than the outer counterpart. This effect can be attributed to the size of the blades and centrifugal forces resulting in swirling with stable vortices. Moreover, the outer swirler plays the role of combustion stabilizer.

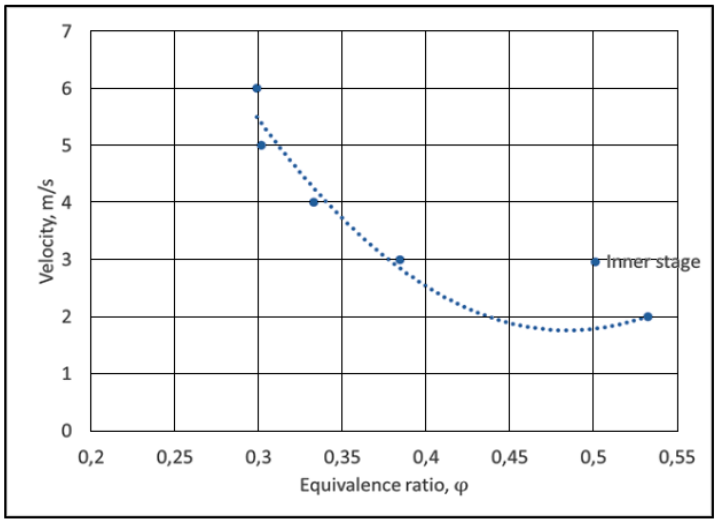

Figure 8. Effect of the air flowrate as a function of the equivalence ratio φ for the inner swirler

Similarly, as it is shown in Fig.9, the same effect can be observed in the outer swirler, but in general, here the combustion process is less stable than in the inner counterpart. The reduced stability can be explained by the greater flow rate than in the inner one, which leads to significant airflow excess. Therefore, it might be decided that the outer swirler has to be started working when the inner one attains its nominal operating regime.

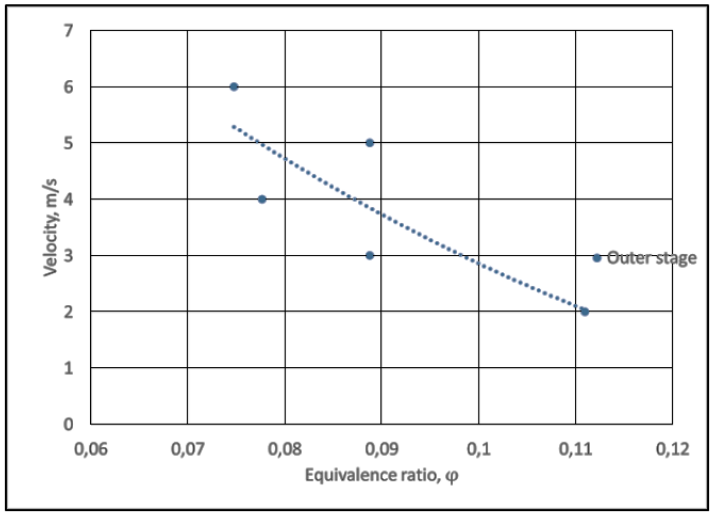

Figure 9. Effect of the airflow rate as a function of the equivalence ratio φ for the outer swirler

The ratio of fuels supply excesses $\varphi_{in}/\varphi_{out}$ as a function of the airflow rate shown in Fig.10, reveals that the stable operating regime can be attained when this ratio is about 4,16 (in average). With the increase in the airflow it reduces down to $\varphi_{in}/\varphi_{out} \approx 4$, but with the decrease in the airflow, it attained a value $\varphi_{in}/\varphi_{out} \approx 4.88$.

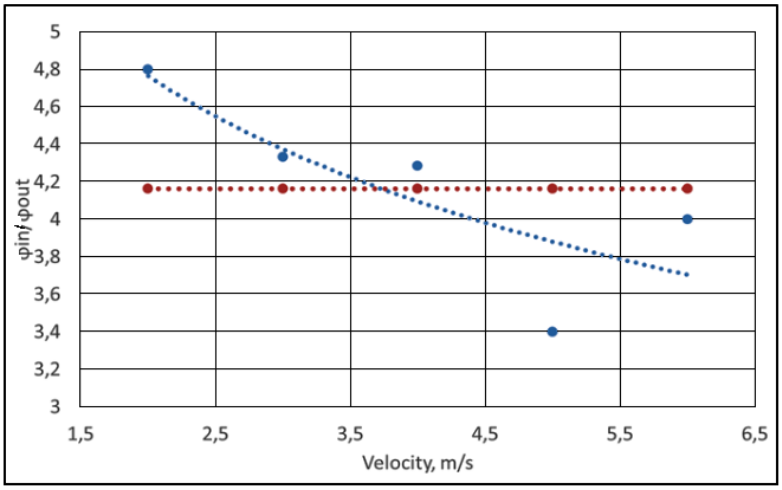

Figure 10. Effect of the airflow rate on the ratio $\varphi_{in}/\varphi_{out}$

The main results of the numerical simulations are summarized in Table 2 and illustrated by Fig. 11 and Fig. 12.

It was established, during the simulation experiments, that the optimal blade angles is 45^{o} based on optimal recirculation of the premixed air-fuel flow. Lower emissions of CO allow attaining a complete combustion process. Table 3 summarized data related to the optimal conditions, established by the numerical simulations, for airflow rate of $4\ m/s$.

Table 3. Numerical simulation results (the best combustion performance)

C, ppm	NO_x	CO	φ
Outer swirler (tier)	1.65	4.28	0.13
Inner swirler (tier)	8.87	3.30	0.15

To determine the optimal blade angle, different angles of the outer and inner tiers were calculated on the software package. The results of calculations are shown in Table 4.

Table 4. Results of calculations the optimal blade angle

inner/outer angles	Concentration of NO_x and CO in combustion products		
	C_{NO_x}, ppm	C_{CO}, ppm	Temterature (K)
30º/30º	7.3045449	0.54361848	1037.0983
30º/45º	11.191727	0.0056578085	1043.0746
45º/30º	19.804627	1.9652161	1041.3074
45º/45º	3.8940556	0.0028665281	1043.6268
60º/30º	8.5767603	24.818512	1034.1566
60º/45º	15.596619	20.176928	1038.0461

Figures 11 and 12 show the temperature fields in some points of the computational area. It follows that the outer swirler has a larger high-temperature zone concerning the inner counterpart and this can be explained by the difference in fuel supplies to these elements of the combustion chamber.

Moreover, the numerical results indicate that the highest temperature of the exhaust gases exists at a distance of about 150 mm behind the frontal surface of the combustor (in both sones of the swirlers). In addition, 300 *mm*, behind the combustor frontal surface, there is a zone of lean combustion around the recirculation zone of the inner swirler. Concerning the outer swirler, this distance is shorter.

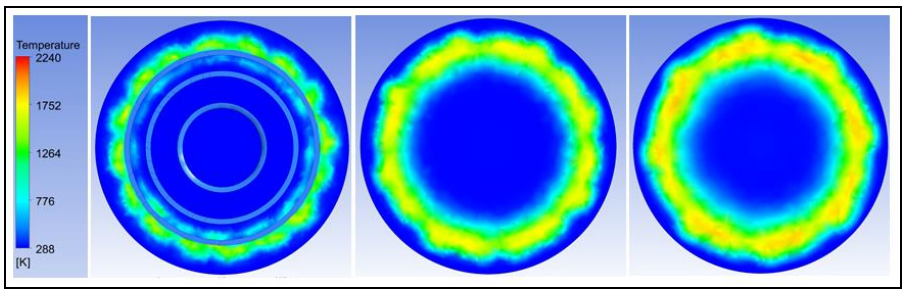

Figure 11. Temperature fields in the outer swiller at different distances from the frontal surface of the combustor: a) at 0 *mm* **; b)- at** 150 *mm* **; c) at at** 300 *mm*

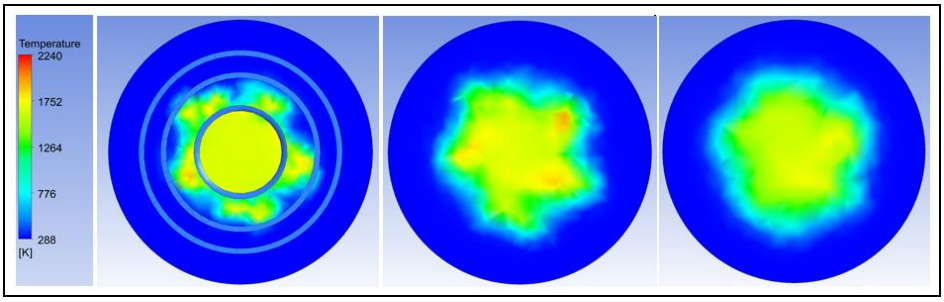

Figure 12. Temperature fields in the inner swiller at different distances from the frontal surface of the combustor: a) at 0 *mm* **; b) at** 150 *mm* **; c) at** 300 *mm*

Conclusions

This research presents experimental results and numerical simulations of double-stage combustion devices with swirler' blade variations allowing control of the combustion process efficiency and NOx emissions.

It was established that the optimal angle of blades assuring optimal flow swirling and performance the combustion process is 45^o.

The lowest emissions of NOx are results of the combustion process in the outer swirler while the lowest concentrations of CO come from the combustion in the inner swirler.

The ratio $\varphi_{in}/\varphi_{out}$ depends on the airflow rate and varies in the range $4-5$. This allows finding the optimal flow rate for each swirler.

The numertical experiments reveal that optimal combustion process depends on the optimal ratio fuel/air and this ration strongly affects the concenatrtions of NOx and CO in the exhaust gases.

Nomenclature

$T_{sim.}$ – temperature on the outlet of the burner (simulation), [K];
T_{exp} - temperature on the outlet of the burner (experimental), [K];
φ – equivalence ratio, [-].

Acknowledgment

This research is funded by the Science Committee of the Ministry of Science and Higher Education of the Republic of Kazakhstan (Grant No. AP14872041).

References

[1] Anufriev, I. S., *et.al.*, Diesel and waste oil combustion in a new steam burner with low NO_X emission, *Fuel, 290* (2021), 120100

[2] Qian, X., *et. al.*, Influence of jet angle on diffusion combustion characteristics and NOx emissions in a self-reflux burner, *Case Studies in Thermal Engineering*, *25* (2021), 100953

[3] Fontanarosa, D., *et. al.*, Combustion performance of a low NOx gas turbine combustor using urea addition into liquid fuel, *Fuel, 288* (2021), 119701

[4] Ti, S., *et. al.*, Effect of outer secondary air vane angles on combustion characteristics and NOx emissions for centrally fuel rich swirl burner in a 600-MWe wall-fired pulverized-coal utility boiler. *Applied Thermal Engineering*, *125* (2017), pp. 951–962

[5] Tao, C., *et.al.*, Effect of carbon dioxide, argon, and helium jets on the synchronous control of combustion instability and NOx emission, *Asia-Pacific Journal of Chemical Engineering*, *16* (2021), pp. 1-14

[6] Dostiyarov, A. M., Results of investigation of the GTE combustion chamber with a two-stage burner, *Espacios, 39* (2019), pp. 15-20

[7] Hussain, M., *et.al.*, A highly diluted oxy-fuel micromixer combustor with hydrogen enrichment for enhancing turndown in gas turbines, *Applied Energy*, *279* (2020), 115818

[8] Abdelhafez, A., *et.al.*, Effects of jet diameter and spacing in a micromixer-like burner for clean oxy-fuel combustion in gas turbines, *Energy, 228* (2021), 120561

[9] Ruan, C., *et.al.*, Experimental study on flame/flow dynamics in a multi-nozzle gas turbine model combustor under thermo-acoustically unstable condition with different swirler configurations, *Aerospace Science and Technology*, *98* (2020), 105692

[10] Ti, S., *et.al.*, Influence of primary air cone length on combustion characteristics and NOx emissions of a swirl burner from a 0.5 MW pulverized coal-fired furnace with air staging, *Applied Energy, 211* (2018), pp. 1179–1189

[11] Wang,Y., *et.al.*, Experimental investigation of the characteristics of NOx emissions with multiple deep air-staged combustion of lean coal, *Fuel, 280* (2020), 118416

[12] Gobbato, P., *et.al.*, Calculation of the flow field and NOx emissions of a gas turbine combustor by a coarse computational fluid dynamics model, *Energy, 45* (2012), 1, pp. 445–455

[13] Tong, Y., *et.al.*, Effects of the position of a bluff-body on the diffusion flames: A combined experimental and numerical study, *Applied Thermal Engineering, 131* (2018), pp. 507–521

[14] Chowdhury B. R., Cetegen B. M., Effects of free stream flow turbulence on blowoff characteristics of bluff-body stabilized premixed flames, *Combustion and Flame, 190* (2018), pp. 302–316

[15] Wu, B., *et.al.*, A numerical investigation of the flame structure and blowoff characteristics of a bluff-body stabilized turbulent premixed flame, *Combustion and Flame, 202* (2019), pp. 376–393

[16] Umyshev, D. R., *et.al.*, Experimental investigation of V-gutter flameholders, *Thermal Science, 21* (2017), 2, pp. 1011–1019

[17] Wang, G., *et.al.*, Experimental investigation of entropy waves generated from acoustically excited premixed swirling flame, *Combustion and Flame, 204* (2019), pp. 85–102

[18] Umyshev, D. R., *et.al.*, Experimental investigation of the management of NOx emissions and their dependence on different types of fuel supply, *Espacios, 38* (2017), 24, Article number 17

[19] Lefebvre , A. H., Ballal, D. R., *Gas turbine combustion: Alternative Fuels and Emissions,* London, Taylor & Francis, 2010. 537 p.

[20] Jin, U., Kim, K. T., Experimental investigation of combustion dynamics and NOx/CO emissions from densely distributed lean-premixed multinozzle CH4/C3H8/H2/air flames, *Combustion and Flame, 229* (2021), 111410

[21] Kharoua, N., *et.al.*, The interaction of confined swirling flow with a conical bluff body: Numerical simulation, *Chemical Engineering Research and Design, 136* (2018), pp. 207–218

[22] Umyshev, D. R., *et.al.*, Experimental investigation of distance between v-gutters onx flame stabilization and NOx emissions, *Thermal Science, 23* (2019), 5B, pp. 2971-2981

[23] Umyshev, D. R., *et.al.*, Effects of different fuel supply types on combustion characteristics behind group of V-gutter flame holders: Experimental and numerical study, *Thermal Science, 24* (2020), pp. 379-391

[24] Hristov, J., *et.al.*, A Novel Vortex Combustion Device Experiments and Numerical Simulations with Emphasis on the Combustion Process and NOx Emissions, *Thermal Science, 26* (2022), 2, pp. 1971–1983

[25] Patent No. 35168, Two-tier Burner 25.06.2021, (Patent na izobreteniye No. 35168, Dvukh Yarusnaya Gorelka), (in rus), 2021

[26] Dostiyarov, A. M., , *et.al.*, Experimental study results of the front-end device with two-tier air burner as part of the gas turbine engine combustion chamber, *Thermal Science*, 27 (2023), 5A, pp. 3709-3718

Received: 18.03.2022.
Revised: 24.02.2024.
Accepted: 22.04.2024.